Ultrafast Dynamics of Highly Conjugated Porphyrin Arrays

Ranjit Kumble, Steven Palese, Victor S.-Y. Lin, Michael J. Therien,* and Robin M. Hochstrasser*

Contribution from the Department of Chemistry, University of Pennsylvania, Philadelphia, Pennsylvania 19104-6323

Received May 26, 1998

Abstract: The photophysical properties of a series of ethynyl-bridged (porphinato)zinc(II) oligomers have been investigated over the femtosecond and picosecond time scales using ultrafast magic angle and polarized pump−probe spectroscopy. Bis[(2,2′,-5,10,15,20-tetraphenylporphinato)zinc(II)]ethyne, bis[(5,5′,-10,20-diphenylporphinato)zinc(II)]ethyne, and 5,15-bis{[(5′,-10′,20′-diphenylporphinato)zinc(II)]ethynyl}[10,20-diphenylporphinato]zinc(II) exhibit rapid (≤150 fs) formation of the emitting state following Soret photoexcitation, nearly an order of magnitude faster than the ∼1 ps $S_2 \rightarrow S_1$ internal conversion observed for a monomeric (porphinato)zinc(II) complex that bears an ethyne moiety fused directly to its macrocycle carbon framework [(5-trimethylsilylethynyl-10,20-diphenylporphinato)zinc(II)]. The femtosecond and picosecond dynamics are strongly influenced by the porphyrin-to-porphyrin linkage topology: bis[(2,2′,-5,10,15,20-tetraphenylporphinato)-zinc(II)]ethyne, in which a β-to-β ethyne bridge links the two (porphinato)zinc(II) moieties, maintains the $x-y$ degeneracy of the emitting state, the dynamics of which are consistent with energy equilibration within a weakly coupled porphyrin pair. In contrast, systems which feature a *meso*-to-*meso* ethynyl-bridged linkage topology between (porphinato)zinc(II) units exhibit properties consistent with significant inter-ring conjugation and loss of $x-y$ degeneracy for the (π, π^*) excited states. Collectively, the steady-state and time-resolved results for these *meso*-to-*meso* bridged systems suggest some degree of conformational heterogeneity for the ground state structures in solution, which differ with respect to the degree of conjugation of porphyrin rings; these conformers interconvert in the S_1 excited state on a ∼30 ps time scale to produce a conformationally uniform, coplanar emitting state.

I. Introduction

An important goal in the development of new solar energy photoconversion schemes is the emulation of the high efficiency characteristic of biological light-harvesting and electron-transfer systems. Numerous biological pigment−protein complexes participating in energy- and charge-transfer processes contain tetrapyrrolic chromophores (chlorophylls, bacteriochlorophylls, bilins) with optical properties appropriate to the prevailing light conditions.[1] The transition energies and oscillator strengths of the chromophores within their protein environments are modulated by interchromophore interactions,[1] as well as by electrostatic[2] and conformational[3] effects, which together serve to engineer specific pathways for thermodynamically favorable migration of excitation or charge; in such processes, the spatial arrangement of the pigments is thought to be of primary importance, particularly with respect to ultrafast energy- and electron-transfer reactions. Although the relative contributions from specific interactions in determining overall mechanism are still debated in certain cases,[1] it is clear that extensive control over the electronic properties of individual chromophores within the biological multipigment assemblies is essential in order to optimize their collective activity.

There is significant interest in the development of (i) multichromophoric assemblies that mimic the photophysics of biological energy transducing systems and (ii) supramolecular entities, inspired by the light-activated properties of these biological models, for potential applications in optoelectronics,[4−6] energy conversion,[7−15] and biomedicine.[16] Considerable effort has been directed toward the syntheses of extended porphyrin

(1) van Grondelle, R.; Dekker, J. P.; Gillbro, T.; Sundstrom, V. *Biochim. Biophys. Acta* **1994**, *1187*, 1−65.

(2) Eccles, J.; Honig, B. *Proc. Natl. Acad. Sci. U.S.A.* **1983**, *80*, 4959−4962.

(3) Gudowska-Nowak, E.; Newton, M. D.; Fajer, J. *J. Phys. Chem* **1990**, *94*, 5795−5801.

(4) (a) LeCours, S. M.; Guan, H.-W.; DiMagno, S. G.; Wang, C. H.; Therien, M. J. *J. Am. Chem. Soc.* **1996**, *118*, 1497−1503. (b) Priyadarshy, S.; Therien, M. J.; Beratan, D. N. *J. Am. Chem. Soc.* **1996**, *118*, 1504−1510. (c) Karki, L.; Vance, F. W.; Hupp, J. T.; LeCours, S. M.; Therien, M. J. *J. Am. Chem. Soc.* **1998**, *120*, 2606−2611.

(5) (a) O'Keefe, G. E.; Denton, G. J.; Harvey, E. J.; Phillips, R. T.; Friend, R. H.; Anderson, H. L. *J. Chem. Phys.* **1996**, *104*, 805−811. (b) Beljonne, D.; O'Keefe, G. E.; Hamer, P. J.; Friend, R. H.; Anderson, H. L.; Brédas, J. L. *J. Chem. Phys.* **1997**, *106*, 9439−9460.

(6) (a) O'Neil, M. P.; Niemczyk, M. P.; Svec, W. A.; Gosztola, D.; Gaines, G. L., III; Wasielewski, M. R. *Science* **1992**, *257*, 63−65. (b) Debreczeny, M. P.; Svec, W. A.; Wasielewski, M. R. *Science* **1996**, *274*, 584−587.

(7) (a) Lin, V. S.-Y.; DiMagno, S. G.; Therien, M. J. *Science* **1994**, *264*, 1105−1111. (b) Lin, V. S.-Y.; Therien, M. J. *Chem. Eur. J.* **1995**, *1*, 645−651.

(8) (a) Wagner, R. W.; Lindsey, J. S.; Seth, J.; Palaniappan, V.; Bocian, D. F. *J. Am. Chem. Soc.* **1996**, *118*, 3996−3997. (b) Hsiao, J.-S.; Krueger, B. P.; Wagner, R. W.; Johnson, T. E.; Delaney, J. K.; Mauzerall, D. C.; Fleming, G. R.; Lindsey, J. S.; Bocian, D. F.; Donohoe, R. J. *J. Am. Chem. Soc.* **1996**, *118*, 11181−11193. (c) Strachan, J.-P.; Gentemann, S.; Seth, J.; Kalsbeck, W. A.; Lindsey, J. S.; Holten, D.; Bocian, D. F. *J. Am. Chem. Soc.* **1997**, *119*, 11191−11201.

(9) (a) Asahi, T.; Ohkohchi, M.; Matsusaka, R.; Mataga, N.; Zhang, R. P.; Osuka, A.; Maruyama, K. *J. Am. Chem. Soc.* **1993**, *115*, 5665−5674. (b) Osuka, A.; Marumo, S.; Mataga, N.; Taniguchi, S.; Okada, T.; Yamazaki, I.; Nishimura, Y.; Ohno, T.; Nozaki, K. *J. Am. Chem. Soc.* **1996**, *118*, 155−168.

(10) (a) Steinberg-Yfrach, G.; Liddell, P. A.; Hung, S.-C.; Moore, A. L.; Gust, D.; Moore, T. A. *Nature* **1997**, *385*, 239−241. (b) Gust, D.; Moore, T. A.; Moore, A. L. *Acc. Chem. Res.* **1993**, *26*, 198−205.

10.1021/ja981811u CCC: $15.00
Published on Web 10/27/1998

arrays for such purposes, employing saturated,[17] aromatic,[18] vinylic,[19] and diphenylacetylenic[8] bridging groups, as well as carbon−carbon single bonds directly linking the macrocycle frameworks of adjacent pigments;[20] these approaches, however, yield oligomeric porphyrin systems with weak exciton coupling and little opportunity to modulate the magnitude of ground- and excited-state electronic interactions between chromophores.

In contrast, a significant improvement in electronic communication between porphyrin pigments can be achieved when ethyne or butadiyne moieties directly link these chromophores at their respective *meso*- or *β*-carbon atoms,[5,7,21−23] It has been demonstrated that when appropriate porphyrinic synthons[7,24] lacking *β*-carbon substituents are utilized as building blocks for either ethyne- or butadiyne-bridged porphyrin arrays that feature a *meso*-to-*meso* linkage topology, novel chromophoric supermolecules are defined which set new benchmarks for ground- and excited-state interpigment electronic coupling in multiporphyrinic assemblies;[7,23] likewise, when such species are utilized as precursors to analogous systems in which porphyrin-pendant *meso*-ethynyl groups are fused to other aromatic entities, unprecedented electronic communication between the ethyne-elaborated aromatic units and the core porphyrin macrocycle is effected.[4,25] Furthermore, a comprehensive series of ethyne- and butadiyne-bridged bis- and tris[(porphinato)zinc(II)] arrays

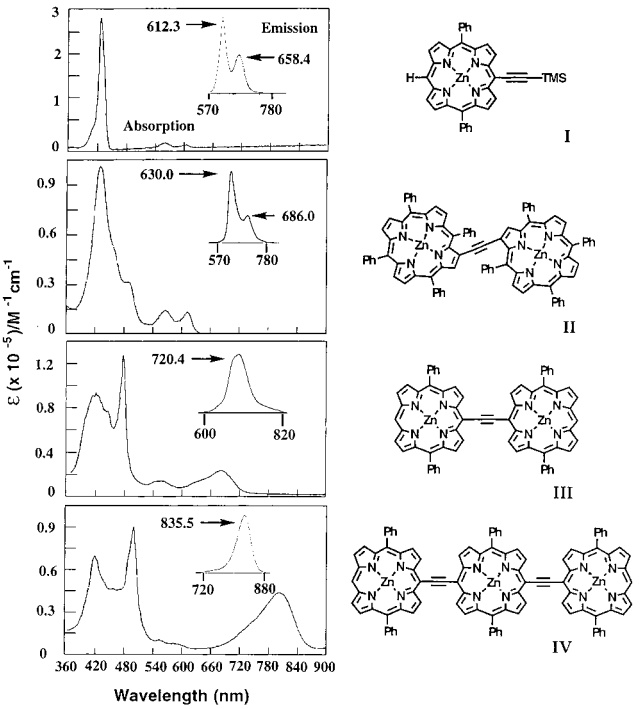

Figure 1. Ambient temperature absorption and fluorescence spectra (insets) for conjugated porphyrins **I**−**IV** recorded in (**I**) $CHCl_3$, (**II**) $CHCl_3$, (**III**) $CHCl_3$, and (**IV**) 10:1 $CHCl_3$−pyridine. See ref 7.

that feature *β*-to-*β*, *meso*-to-*β*, and *meso*-to-*meso* linkage topologies for these cylindrically *π*-symmetric groups evince that remarkable modulation of the degree of excitonic and electronic coupling between the component porphyrin macrocycles is possible.[7,23] The ability to tune these types of couplings translates into the capacity to significantly engineer supramolecular chromophoric properties and thus ultimately design new photophysical entities. Figure 1 shows the chemical structures of an ethyne-elaborated (porphinato)zinc(II) monomer, (5-trimethylsilylethynyl-10,20-diphenylporphinato)zinc(II) (**I**), two ethyne-bridged porphyrin dimers, bis[(2,2′,-5,10,15,20-tetraphenylporphinato)zinc(II)]ethyne (**II**) and bis[(5,5′,-10,20-diphenylporphinato)zinc(II)]ethyne (**III**), and 5,15-bis{[(5′,-10′,20′-diphenylporphinato)zinc(II)]ethynyl}[10,20-diphenylporphinato]zinc(II) (**IV**), a tris(porphinato)zinc(II) complex in which two ethyne moieties connect three (10,20-diphenylporphinato)zinc(II) macrocycles at their respective *meso*-carbon positions. The steady-state absorption and fluorescence spectra displayed in Figure 1 illustrate (i) the disparate absorptive and emissive properties of conjugated arrays **II**−**IV** with respect to an ethyne-derivatized (porphinato)zinc(II) monomer, **I**, and (ii) the sharp topological dependence of both the ground- and excited-state electronic interactions, evident in the associated spectra displayed for *β*-to-*β* bridged **II** and *meso*-to-*meso* linked **III**.[7]

The eventual incorporation of these and related highly conjugated multiporphyrin structures into a next generation of photosynthetic biomimetics or optoelectronic materials requires a thorough knowledge of the excited-state dynamics of these systems. In the present study, we apply femtosecond pump−probe spectroscopy to investigate the isotropic and anisotropic transient dynamics of compounds **I**−**IV** on subpicosecond and picosecond time scales. We utilize magic angle transient dynamical studies to investigate population relaxation dynamics

(11) (a) Gaines, G. L., III; O'Neil, M. P.; Svec, W. A.; Niemczyk, M. P.; Wasielewski, M. R. *J. Am. Chem. Soc.* **1991**, *113*, 719−721. (b) Wasielewski, M. R.; Gaines, G. L., III; Wiederrecht, G. P.; Svec, W. A.; Niemczyk, M. P. *J. Am. Chem. Soc.* **1993**, *115*, 10442−10443.

(12) Joran, A.D.; Leland, B. A.; Felker, P. M.; Zewail, A. H.; Hopfield, J. J.; Dervan, P. B. *Nature* **1987**, *327*, 508−511.

(13) Helms, A.; Heiler, D.; McLendon, G. *J. Am. Chem. Soc.* **1992**, *114*, 6227−6238.

(14) Harriman, A.; Odobel, F.; Sauvage, J.-P. *J. Am. Chem. Soc.* **1995**, *117*, 9461−9472.

(15) (a) Rodriquez, J.; Kirmaier, C.; Johnson, M. R.; Friesner, R. A.; Holten, D.; Sessler, J. L. *J. Am. Chem. Soc.* **1991**, *113*, 1652−1659. (b) Sessler, J. L.; Wang, B.; Harriman, A. *J. Am. Chem. Soc.* **1993**, *115*, 10418−10419.

(16) *Photodynamic Therapy of Neoplastic Disease*; Kessel, D., Ed.; CRC Press: Boca Raton, FL, 1990; Vols. I, II.

(17) (a) Selensky, R.; Holten, D.; Windsor, M. W.; Paine, J. B., III; Dolphin, D. *Chem. Phys.* **1981**, *60*, 33−46. (b) Kamogawa, H.; Miyama, S.; Minoura, S. *Macromolecules* **1989**, *22*, 2123−2126. (c) Fleischer, E. B.; Shachter, A. M. *J. Heterocycl. Chem.* **1991**, *28*, 1693−1699. (d) Scamporrino, E.; Vitalini, D. *Macromolecules* **1992**, *25*, 1625−1632.

(18) (a) Tabushi, I.; Sasaki, T. *Tetrahedron Lett.* **1982**, 1913−1916. (b) Chang, C. K.; Abdalmuhdi, I. *J. Org. Chem.* **1983**, *48*, 5388−5390. (c) Sessler, J. L.; Hugdall, J.; Johnson, M. R. *J. Org. Chem.* **1986**, *51*, 2838−2840. (d) Heiler, D.; McLendon, G.; Rogalskyj, P. *J. Am. Chem. Soc.* **1987**, *109*, 604−606. (e) Sessler, J. L.; Johnson, M. R.; Lin, T.-Y.; Creager, S. E. *J. Am. Chem. Soc.* **1988**, *110*, 3659−3661. (f) Osuka, A.; Maruyama, K. *J. Am. Chem. Soc.* **1988**, *110*, 4454−4456. (g) Meier, H.; Kobuke, Y.; Kugimiya, S. *J. Chem. Soc., Chem. Commun.* **1989**, 923. (h) Nagata, T.; Osuka, A.; Maruyama, K. *J. Am. Chem. Soc.* **1990**, *112*, 3054−3059. (i) Helms, A.; Heiler, D.; McLendon, G. *J. Am. Chem. Soc.* **1991**, *113*, 4325−4327. (j) Osuka, A.; Nakajima, S.; Nagata, T.; Muruyama, K.; Toriumi, K. *Angew. Chem., Int. Ed. Engl.* **1991**, *30*, 582−584.

(19) (a) Vicente, M. G. H.; Smith, K. M. *J. Org. Chem.* **1991**, 56, 4407−4418. (b) Burrelll, K.; Officer, D. L. ; Reid, D. C. W. *Angew. Chem., Int. Ed. Engl.* **1995**, *34*, 900−902. (c) Arnold, D. P.; Borovkov, V. V.; Ponomarev, G. V. *Chem. Lett.* **1996**, 485−486. (d) Higuchi, H.; Takeuchi, M.; Ojima, J. *Chem. Lett.* **1996**, 593−594.

(20) (a) Susumu, K.; Shimidzu, T.; Tanaka, K.; Segawa, H. *Tetrahedron Lett.* **1996**, *37*, 8399−8402. (b) Osuka, A.; Shimidzu, H. *Angew. Chem., Int. Ed. Engl.* **1997**, *36*, 135−137. (c) Khoury, R. G.; Jaquinod, L.; Smith, K. M. *Chem. Commun.* **1997**, 1057−1058.

(21) (a) Arnold, D. P.; Nitschinsk, L. J. *Tetrahedron* **1992**, *48*, 8781−8792. (b) Arnold, D. P.; Heath, G. A. *J. Am. Chem. Soc.* **1993**, *115*, 12197−12198.

(22) Anderson, H. L. *Inorg. Chem.* **1994**, *33*, 972−981.

(23) (a) Angiolillo, P. J.; Lin, V. S.-Y.; Vanderkooi, J. M.; Therien, M. J. *J. Am. Chem. Soc.* **1995**, *117*, 12514−12527. (b) Lin, V. S.-Y.; Williams, S. A.; Therien, M. J. Manuscript in preparation.

(24) (a) DiMagno, S. G.; Lin, V. S.-Y.; Therien, M. J. *J. Am. Chem. Soc.* **1993**, *115*, 2513−2515. (b) DiMagno, S. G.; Lin, V. S.-Y.; Therien, M. J. *J. Org. Chem.* **1993**, *58*, 5983−5993.

(25) (a) LeCours, S. M.; DiMagno, S. G.; Therien, M. J. *J. Am. Chem. Soc.* **1996**, *118*, 11854−11864. (b) LeCours, S. M.; Phillips, C. M.; dePaula, J. C.; Therien, M. J. *J. Am. Chem. Soc.* **1997**, *119*, 12578−12589.

between and within optically accessible (π, π^*) excited states, and polarized, time-resolved optical spectroscopic measurements to probe equilibration and energy-transfer processes. Central themes of this work include delineating how the conjugated linkage topology impacts the nature of the initially prepared excited state and the time dependence of the ultrafast spectral evolution in these ethyne-bridged bis- and tris(porphinato)-zinc(II) systems.

II. Experimental Methods

II.a. Materials. The syntheses of compounds **I**, **II**, **III**, and **IV** have been previously reported.[7] For transient optical studies, the (porphinato)zinc(II) complexes were dried under vacuum, dissolved in the appropriate solvent, and transferred under nitrogen to a Schlenk-style fluorescence cell in order to continuously maintain an inert atmosphere throughout the experiment. Sample concentrations ranged between 1 and 3 μM and were determined by electronic absorption spectroscopy by using the known extinction coefficients of the compounds; concentrations in this range gave absolute absorbances between 0.6 and 0.8 AU at the pump wavelength. Solvents utilized in this work were obtained from Fisher Scientific (HPLC Grade). Dry, deoxygenated solvents were used in the pump−probe spectroscopic experiments; DMF was predried over 4-Å molecular sieves, and then distilled from anhydrous calcium hydride under vacuum, while $CHCl_3$ was distilled from CaH_2 under N_2. Figure 1 shows the absorbance and fluorescence emission spectra for compounds **I**−**III** in $CHCl_3$ and compound **IV** in 10:1 $CHCl_3$−pyridine. The transient optical data for compounds **I** and **II** and (5,10,15,20-tetraphenylporphinato)zinc(II) were obtained in $CHCl_3$ solvent, while DMF was used for complexes **III** and **IV**; under the conditions of these experiments (*vide infra*), no photodecomposition of any of these chromophores was observed. The prominent optical spectroscopic features observed for compounds **III** and **IV** in DMF differ little from that displayed in Figure 1.

II.b. Femtosecond Laser Apparatus. A mode-locked Ti:sapphire laser (built according to the design of Asaki and co-workers)[26] was used to produce laser pulses of 20 fs duration (FWHM) centered at 800 nm (84 MHz repetition rate). These pulses were stretched to ~66 ps in a grating stretcher and amplified at 3 kHz using a Ti:sapphire regenerative amplifier pumped by the second harmonic (527 nm, 8.5 W) from an intracavity-doubled, Q-switched Nd:YLF laser (Quantronix 527). Compression of the amplified pulses yielded 75−100 μJ pulses centered at 800 nm having a full width at half-maximum (FWHM) of 35 fs. Details concerning the design of the grating stretcher and compressor and Ti:sapphire regenerative amplifier have been given previously.[27,28] The measurements described here employed photo-excitation at either the Ti:sapphire fundamental (800 nm) frequency or the second harmonic (400 nm) frequency which was generated in a 100 μm BBO crystal; excitation energies of 50−75 nJ were used. For two-color measurements, 1 μJ 800 nm pulses were used to generate continuum in a 1 mm sapphire window (Meller Optics, c-cut), and the appropriate probe wavelengths were selected using interference filters (Corion, 10 nm bandpass). Relative polarizations of pump and probe pulses were adjusted using an achromatic half-waveplate to rotate the pump beam polarization. Measurements were conducted with pump and probe polarizations in parallel (0°) and perpendicular (90°) orientations for anisotropy determination, and at the magic angle (54.7°) to follow isotropic dynamics. Excitation pulses were chopped at 1.45 kHz, and the temporal delay between pump and probe pulses was controlled using a variable delay line in the probe beam path. The two beams were focused onto the sample (contained in a 1 mm path length Schlenk-style optical cell that continuously maintained an inert atmosphere throughout the course of the experiment) and spatially overlapped using a near-colinear geometry. The transmitted probe intensity was detected with a silicon photodiode, the output from which was processed with a boxcar (Stanford Instruments) and digitized for computation of the absorption difference signal. The instrument response function (IRF) was assumed to be Gaussian; its FWHM was determined from the rise of the pump−probe signal from a solution of IR 140 dye or a poly(phenylvinylene) (PPV) sample. For experiments involving an 800 nm excitation wavelength (λ_{ex}), the width of the IRF was found to be in the range of 50−100 fs, and 120−150 fs for λ_{ex} = 400 nm. Pump−probe signals were fit to convolutions of the IRF with a sum of exponentials, each with a time constant, τ_i, and an amplitude, a_i, which is positive for transient absorption and negative for transient gain and bleach signals.

The anisotropy $r(t)$, obtained from the parallel ($I_{||}$) and perpendicular ($I_{\perp}$) transient signals, is given by

$$r(t) = (I_{||} - I_{\perp})/(I_{||} + 2I_{\perp}) \quad (1)$$

The parallel and perpendicular signals were simultaneously fit to convolutions of the instrument response with appropriate functions representing the true magic angle signal and anisotropy, each modeled by a sum of exponentials.[29] On time scales of hundreds of picoseconds and longer, time constants representing the intrinsic lifetime of the emitting state were held fixed at the values determined from time-correlated single photon counting (TCSPC) measurements.[23b] Our fits examined anisotropy decays occurring on time scales faster than 10 ps, and it was assumed that a constant anisotropy value [$r(\infty)$] is established at long times. The eventual complete depolarization of signals due to rotational diffusion was not considered here, which has been determined to occur for these compounds on much longer time scales (75−500 ps).[23b]

III. Results

III.a. Excited-State Dynamics of Benchmark (Porphinato)zinc(II) Complexes. The magic angle and anisotropic transient dynamics of two (porphinato)zinc(II) monomers, (5,10,15,20-tetraphenylporphinato)zinc(II) (**ZnTPP**) and (5-trimethylsilylethynyl-10,20-diphenylporphinato)zinc(II) (**I**), were examined using 400 nm excitation; as expected for porphyrin singlet excited states,[30] the difference signal is dominated by transient absorption in the 600−650 nm spectral region for both compounds. On ultrafast time scales, an instantaneous rise of the transient absorption and a subsequent decay (τ = 0.9 ps) are seen for I (Figure 2). Excitation at 400 nm populates the S_2 (π, π^*) porphyrin excited state, which subsequently decays by efficient internal conversion to the lower energy S_1 (π, π^*) state. The observed signals thus reflect initial absorption from the S_2 state and subsequent nonradiative $S_2 \rightarrow S_1$ relaxation on a ~1 ps time scale. In the case of **ZnTPP**, a 1.2 ps time constant for internal conversion was determined from these experiments, which is similar to the 2−4 ps values reported for this process that were obtained from steady-state[31] and time-resolved[32] analysis of emission from the S_2 state. On longer time scales (Supporting Information), the S_1 transient absorption signal decays slowly due to the intrinsic (>1 ns) excited-state lifetime and exhibits a weak 18 ps component which is evident at 610 nm. This decay is consistent with vibrational cooling within the S_1 excited state which is expected to occur on a 10−20 ps time scale.[30]

(26) Asaki, M. T.; Huang, C.-P.; Garvey, D.; Zhou, J.; Kapteyn, H. C.; Murnane, M. M. *Opt. Lett.* **1993**, *18*, 977−979.

(27) Wynne, K.; Reid, G. D.; Hochstrasser, R. M. *Opt. Lett.* **1994**, *19*, 895−897.

(28) Kumble, R.; Palese, S.; Visschers, R. W.; Dutton, P. L.; Hochstrasser, R. M. *Chem. Phys. Lett.* **1996**, *261*, 396−404.

(29) (a) Galli, C.; Wynne, K.; LeCours, S. M.; Therien, M. J.; Hochstrasser, R. M. *Chem. Phys. Lett.* **1993**, *206*, 493−499. (b) Wynne, K.; LeCours, S. M.; Galli, C.; Therien, M. J.; Hochstrasser, R. M. *J. Am. Chem. Soc.* **1995**, *117*, 3749−3753.

(30) Rodriguez, J.; Kirmaier, C.; Holten, D. *J. Am. Chem. Soc.* **1989**, *111*, 6500−6506.

(31) Kobayashi, H.; Kaizu, Y. In *Porphyrins: Excited States and Dynamics*; Gouterman, M., Rentzepis, P., Straub, K. D., Eds.; American Chemical Society Symposium Series *321*; American Chemical Society: Washington, DC, 1986; p 105.

(32) Chosrowjan, H.; Tanigichi, S.; Okada, T.; Takagi, S.; Arai, T.; Tokumaru, K. *Chem. Phys. Lett.* **1995**, *242*, 644−649.

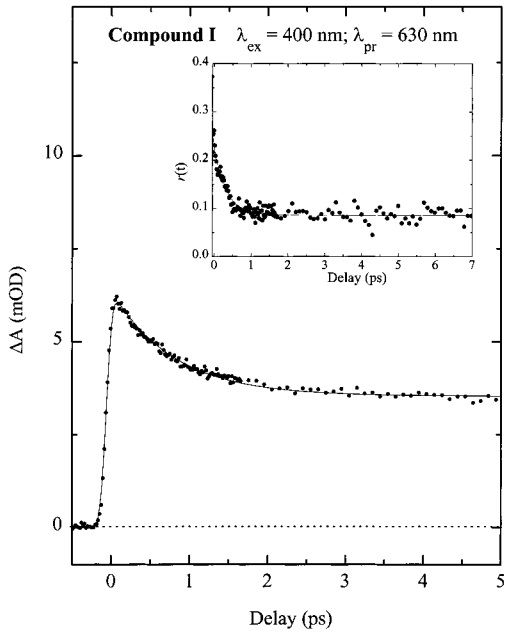

Figure 2. Magic angle transient signal and anisotropy (inset) for *meso*-ethynyl elaborated (5,15-diphenylporphinato)zinc(II) (**I**) following 400 nm excitation. The dashed line indicates the position of the zero difference signal while the positive signal denotes transient absorption; time constants and normalized amplitudes (in parentheses) are as follows: $\tau_1 = 0.9$ ps (0.43), $\tau_2 = 2.2$ ns (0.57).

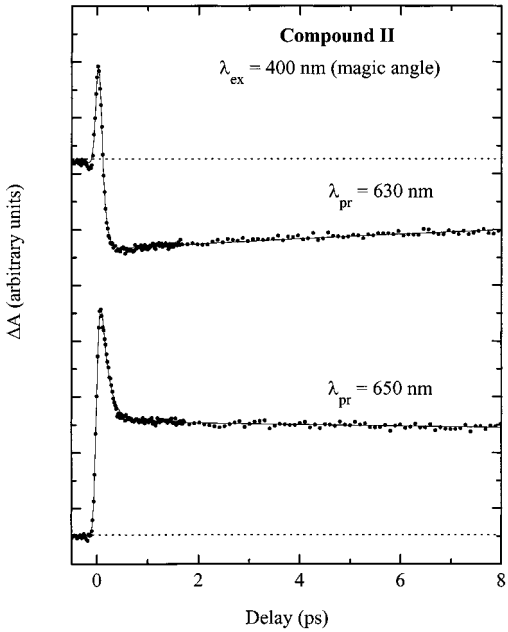

Figure 3. Magic angle transient signal probed at 630 and 650 nm for the β-to-β ethyne-bridged dimer (**II**) following 400 nm excitation; data fits are displayed as solid lines. At 630 nm, $\tau_1 = 0.03$ ps (0.9), $\tau_2 = 18$ ps (−0.06), $\tau_2 = 1.6$ ns (−0.04). At 650 nm, $\tau_1 = 0.15$ ps (0.65), $\tau_2 = 18$ ps (0.06), $\tau_3 = 1.6$ ns (0.29).

The anisotropic transient dynamics for compound **I** are shown in Figure 2 (inset). A single-exponential ($\tau = 350$ fs) depolarization of the transient absorption signal is observed from an initial value $r(0) = 0.25$ to a final value [$r(\infty)$] of 0.07; similar behavior was observed for **ZnTPP** ($\tau = 400$ fs, $r(0) = 0.28$, $r(\infty) = 0.08$; data not shown). The magnitude of this time constant is consistent with equilibration of an incoherent S_2 state having a nonstatistical mixture of near degenerate B_x and B_y components, which leads to a final anisotropy value of ~0.1 as the initial population becomes randomized between the orthogonal states.[29,33,34] The initial anisotropy is lower than the expected value of 0.4 for these complexes, possibly a consequence of accessing transitions with the probe pulse with different anisotropies.[34] Previous studies[30] have located a manifold of states which lie 35000−45000 cm^{-1} above the ground state; transitions to these states are strongly allowed from the E_u symmetric S_1 state. Because the S_2 and S_1 states have identical symmetry, it is further expected that strong overlapping absorption bands from the S_2 state to these higher states will be observed in the 600−700 nm spectral region.[34]

III.b. Ethyne-Bridged Bis[(porphinato)zinc(II)] Chromophores. Pump−probe measurements carried out on the β-to-β ethynyl-bridged dimer **II** employing 400 nm excitation reveal fast dynamics in the 600−650 nm region (Figure 3): a pulse width-limited ($\tau < 70$ fs) component is observed at 630 nm, where photobleaching dominates the difference signal, and a 150 fs decay of transient absorption is seen at 650 nm. It is likely that the 150 fs component reflects relaxation to the S_1 excited state, while the pulse width-limited feature ($\tau < 100$ fs) at 630 nm likely represents a two-photon absorption resonant with a higher lying S state. At longer delay (see the Supporting Information), an 18 ps component is observed at 630 nm, consistent with the time scale for vibrational cooling in the S_1 state.[30] Slower decay of the difference signal at both wavelengths occurs due to population decay from the S_1 state ($\tau >$ 1 ns). The anisotropic transient dynamics reveal biphasic decay on subpicosecond time scales (Figure 4) from an initial value of 0.36 to a final value of ~0.05 with time constants of $\tau_1 =$ 150 fs and $\tau_2 = 650$ fs.

For the *meso*-to-*meso* ethyne-bridged bis[(porphinato)zinc(II)] complex (**III**), the difference signal rises instantaneously in the 650−800 nm spectral region (Figure 5). The difference signal is negative across this entire spectral range, representing contributions from bleaching of the ground-state absorption and emission from the excited state. Although instantaneous ground-state photobleaching is expected to follow Soret photoexcitation, the rise of the difference signal is immediate within the time resolution of these measurements even at longer wavelengths (720−770 nm), where emission dominates the spectrum. These results strongly suggest ultrafast formation of the emitting state on a time scale which lies outside the resolution of this experiment ($\tau < 100$ fs). An additional, smaller component is observed at 720 nm with a time constant of 700 fs: the origin of this component will be discussed in further detail in the Discussion. Figure 6 shows the magic angle transient kinetics at longer delays. It is evident from the data that the difference signal for the *meso*-to-*meso* ethyne-bridged dimer continues to evolve past 10 ps for probe wavelengths of 720 and 770 nm: a 31 ps component is present which appears as a decay of the signal at shorter wavelength and a rise at longer wavelength. These results demonstrate a slow red shift of **III**'s emission on a time scale which is longer than is typical for excited-state vibrational relaxation in porphyrins.

In contrast to the anisotropic dynamics observed for β-to-β ethyne-bridged **II**, the fluorescence anisotropy measured for compound **III** exhibits a constant value of ~−0.12 for all probe

(33) Wynne, K.; Hochstrasser, R. M. *Chem. Phys.* **1993**, *171*, 179−188.

(34) The transient absorption anisotropy from a dephased, nonequilibrated population (r_d) within an E-symmetry state will depend upon the symmetry of the resonant higher state. This specific case has been considered in ref 33, where it was shown that r_d is expected to take on a value of 0.4 for A_1 or B_1 states and −0.2 for A_2 or B_2 states; intermediate values can therefore result if overlapping bands are present at the probe wavelength. The equilibrated anisotropy (r_e) is 0.1 in all cases (see ref 33).

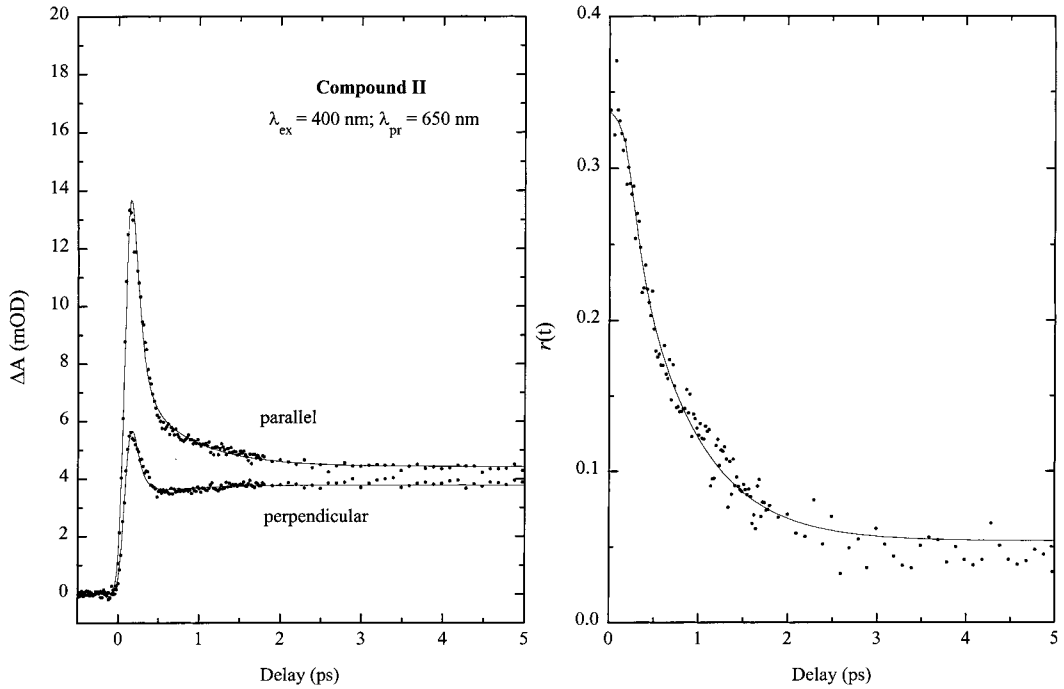

Figure 4. Anisotropic transient dynamics of the β-to-β ethyne-bridged dimer (**II**) probed at 650 nm following 400 nm excitation. (A) Comparison of difference signals for parallel and perpendicular relative orientation of pump and probe polarization and fits to each (solid lines). (B) Time dependence of the anisotropy; the fit is shown as a solid line. ($r_1 = 0.04$, $\tau_1 = 0.15$ ps, $r_2 = 0.27$, $\tau_2 = 0.65$ ps, $r(\infty) = 0.05$.

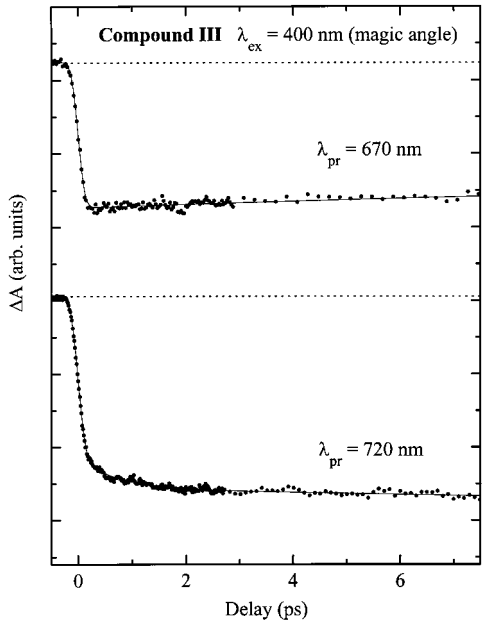

Figure 5. Magic angle transient signal for the *meso*-to-*meso* ethyne-bridged dimer (**III**) probed at 670 and 720 nm following 400 nm excitation; fits of the experimental data are displayed as solid lines. At 670 nm, $\tau_1 = 31$ ps (-0.35), $\tau_2 = 1.2$ ns (-0.65). At 720 nm, $\tau_1 = 0.7$ ps (0.1), $\tau_2 = 31$ ps (0.15), $\tau_3 = 1.2$ ns (-0.75).

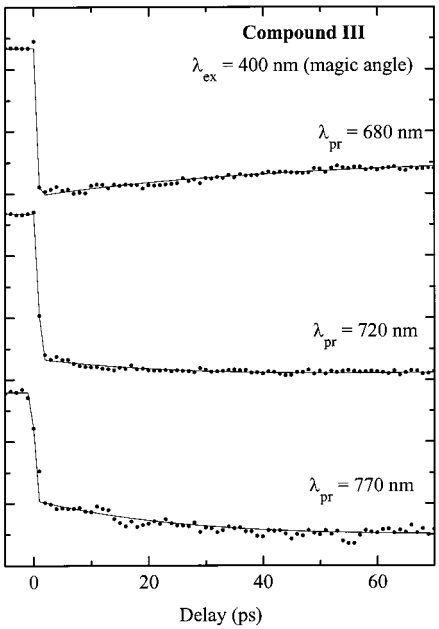

Figure 6. Picosecond isotropic transient dynamics and fits (solid lines) for compound **III** following 400 nm excitation at specified probe wavelengths (λ_{pr}). At 720 nm, the fit parameters are the same as in Figure 5. At 770 nm, $\tau_1 = 31$ ps (0.24), $\tau_2 = 1.2$ ns (-0.76).

wavelengths across the 650−770 nm range on a subpicosecond time scale (Supporting Information). Photoexcitation of the conjugated porphyrin dimer that features a *meso*-to-*meso* linkage topology at 400 nm thus accesses a state which is polarized orthogonal to the $S_0 \rightarrow S_1$ transition probed at 720 nm. The absorption spectrum of compound **III** (Figure 1) is consistent with the presence of several overlapping transitions in the Soret region, thus serving as the likely cause of this deviation from the expected fluorescence anisotropy value for a perpendicular transition moment (-0.2). Equilibration dynamics, similar to that seen for the monomeric (porphinato)zinc(II) complexes (**ZnTPP** and **I**) and the β-to-β ethyne-bridged dimer appear to be absent, indicating that the $x-y$ degeneracy of the emitting state has been removed.

III.c. Excited-State Dynamics of a Tris(Porphinato)-zinc(II) Complex Featuring a *meso*-to-*meso* Ethynyl Linkage Topology. Excitation of the *meso*-to-*meso* ethynyl-linked (porphinato)zinc(II) trimer (**IV**) at 400 nm leads to isotropic and anisotropic dynamics which are quite similar to those observed for the *meso*-to-*meso* ethyne-bridged dimer (**III**). The difference signal at early time in the 700−900 nm region is again dominated by contributions from bleaching and transient

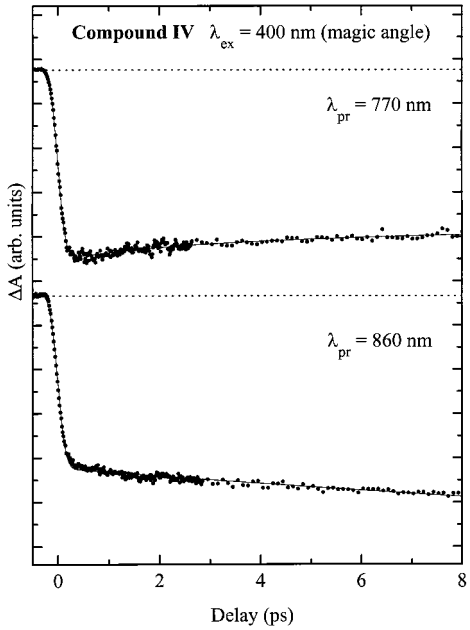

Figure 7. Magic angle transient signal obtained at 770 and 860 nm for the *meso*-to-*meso* ethyne-bridged trimer (**IV**) following 400 nm excitation; fits to the data are shown as solid lines. At 770 nm, $\tau_1 = 3$ ps (−0.08), $\tau_2 = 35$ ps (0.24), $\tau_3 = 0.9$ ns (−0.68). At 860 nm, $\tau_1 = 35$ ps (0.32), $\tau_2 = 0.9$ ns (−0.68).

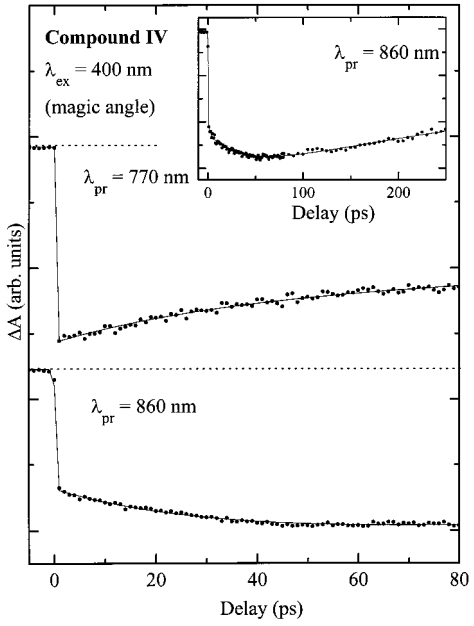

Figure 8. Picosecond isotropic transient dynamics and fits (solid lines) for the *meso*-to-*meso* ethyne-bridged trimer (**IV**) following 400 nm excitation at specified probe wavelengths (λ_{pr}). Fit parameters are the same as in Figure 7. Inset: transient signal at >100 ps delay (λ_{pr} = 860 nm).

gain (stimulated emission), which rises instantaneously at all wavelengths probed in this region (Figure 7). Thus, as was observed for **III**, the formation of the emitting state for this conjugated tris[(porphinato)zinc(II)] complex is complete within the time resolution of these measurements (τ < 100 fs). Following this initial growth, the signal exhibits a 3 ps rising component at 770 nm and a slower 35 ps decay (Figure 7), which appears as a rise at longer wavelength; note that, at 860 nm, the signal grows and then decays slowly with the intrinsic lifetime of the emitting state (Figure 8, inset). Thus, a slow red shift of the emission is seen which is similar to that observed for the *meso*-to-*meso* bridged dimer **III**. Interestingly, dynamics on this 35 ps time scale are *absent* when direct excitation of the emitting state at 800 nm (Figure 9) is carried out: instead, a fast dynamic red shift of the emission is observed which exhibits biexponential kinetics ($\tau_1 = 150$ fs, $\tau_2 = 2.5$ ps), and features no other slower kinetic components detectable on time scales less than 100 ps. The time scale and biphasic nature of the fast red shift suggest that it reflects solvation dynamics, with the 150 fs and 2.5 ps components representing reorganization along respective inertial and diffusive solvent coordinates.[35]

Finally, comparison of the pump−probe anisotropies for 400 and 800 nm excitation of the ethyne-linked tris[(porphinato)-zinc(II)] assembly (Supporting Information) is consistent with the dynamical description formulated for compound **III**, and confirms the nondegenerate nature of the *x*- and *y*-polarized transitions for the S_1- and S_2-excited states of oligomeric (porphinato)zinc(II) species that feature a *meso*-to-*meso* ethyne-bridged linkage topology. For 400 nm excitation, the anisotropy measured probing at 800 nm ($r = -0.07$) reveals the orthogonality between these two electronic transitions, again consistent with that found for the *meso*-to-*meso* ethyne-bridged dimer. For excitation at 800 nm, the anisotropy measured probing at 870 nm ($r = 0.38$) indicates that the pumped and probed transitions are parallel, and that unlike that observed for **ZnTPP**, **I**, and **II**, the emitting state is nondegenerate. No dynamics suggestive of *x*−*y* interconversion are observed, providing further support for significant splitting between the Q_x- and Q_y-components of the S_1 excited state.

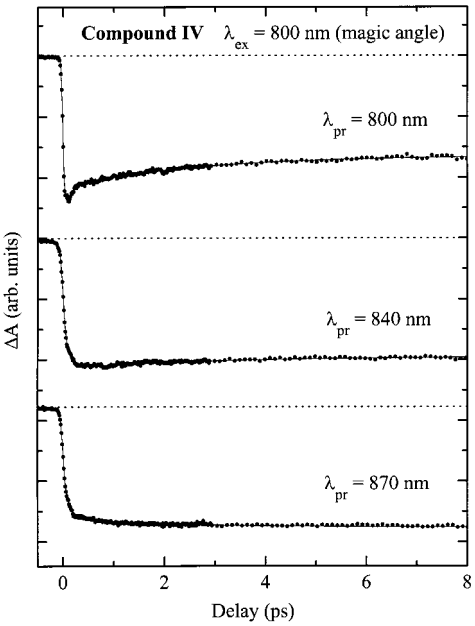

Figure 9. Magic angle transient signal observed at specified probe wavelengths (λ_{pr}) following 800 nm excitation for the *meso*-to-*meso* ethyne-bridged trimer (**IV**); fits of the experimental data are displayed as solid lines. At 800 nm, $\tau_1 = 0.15$ ps (−0.16), $\tau_2 = 2.5$ ps (−0.19), $\tau_3 = 0.9$ ns (−0.65). At 840 nm, $\tau_1 = 0.15$ ps (0.2), $\tau_2 = 2.5$ ps (−0.06), $\tau_3 = 0.9$ ns (−0.74). At 870 nm, $\tau_1 = 0.15$ ps (0.2), $\tau_2 = 2.5$ ps (0.05), $\tau_3 = 0.9$ ns (−0.75).

IV. Discussion

IV.a. Ethynyl Linkage Topology and the Nature of Interchromophore Electronic Interactions. In order to

(35) Horng, M. L.; Gardecki, J. A.; Papazyan, A.; Maroncelli, M. *J. Phys. Chem.* **1995**, *99*, 17311−17337.

rationalize the optical properties of ethynyl-bridged (porphinato)zinc(II) systems **II**−**IV**, it is necessary to consider in detail the interplay between the range of sterically accessible chromophore−chromophore dihedral angles at ambient temperature and the impact that porphyrin-to-porphyrin linkage topology has upon ground- and excited-state electronic coupling.[7] A β-to-β ethyne bridge enforces a large dihedral angle between **II**'s constituent 5,10,15,20-tetraphenylporphinato)zinc(II) pigments; the calculated minimum energy torsional angle for this species resides at 80°, and substantial steric congestion caused by relative positioning of 20-phenyl rings with respect to the two porphyrin macrocycles results in nesting of the dihedral angle-dependent potential energy surface about this minimum.[7b] While this near-orthogonal orientation of the (porphinato)zinc(II) units of the dimer restricts inter-ring ground-state conjugation, it allows for mixing of the electronic states of each monomer by excitonic interactions. These interactions are more significant in the Soret region due to the large transition dipole moment associated with these transitions and are manifest in the pronounced spectral splitting observed over the 390−500 nm energy domain (Figure 1); note that the absorption bands for the Q-states resemble those of an isolated **ZnTPP** monomer,[7] indicative of the fact that the lowest lying singlet electronic excited states of the β-to-β ethyne-bridged dimer are weakly-coupled, localized excited states, which preserve the $x-y$ degeneracy associated with the emitting state of each monomer.

In contrast, both static and dynamic optical data are consistent with the fact that the *meso*-to-*meso* connectivity highlighted in compounds **III** and **IV** facilitates substantial electronic interactions between porphyrin pigments when cylindrically π-symmetric ethyne moieties are exploited as the chromophoric linkers.[7,23] This enhanced porphyrin−porphyrin coupling derives from two factors: (i) Elementary electronic structure considerations predict that, for a fixed porphyrin−porphyrin torsional angle, the magnitude of electronic coupling facilitated by cylindrically π-symmetric porphyrin-to-porphyrin linking groups should follow the order *meso*-to-*meso* > *meso*-to-β > β-to-β; this expectation has been borne out experimentally in the absorptive and emissive properties of a series of butadiynyl-bridged bis(porphyrin) systems possessing similar torsional barriers to rotation.[7b] (ii) With respect to β-to-β ethyne-bridged **II**, the barrier to rotation about the ethyne linker for *meso*-to-*meso* ethyne-bridged **III** and **IV** is minimal.[7b,36] These facts coupled with the large body of spectroscopic evidence[4,7,23,25] that suggest that compounds **III**, **IV**, and similar species possess at least some ground-state charge resonance character argue strongly for the supposition that substantial populations of conformers at ambient temperature exist in which the (porphinato)zinc(II) components of these arrays have maximal or near-maximal conjugation. Indeed, the pronounced intensification and red shift of the lowest energy absorption bands observed for the *meso*-to-*meso* ethyne-bridged dimer and trimer are consistent with such increased conjugation, stabilizing transitions which are polarized along the long axis of these molecules;[7] INDO electronic structure calculations further support this description of the ground and low-lying singlet excited states of compounds **III** and **IV**.[37]

In addition to the significant red shift of the lowest energy absorption bands of the *meso*-to-*meso* ethyne-bridged dimer and trimer, these bands display a pronounced asymmetry which deserves special comment. X-ray crystallographic studies of a *meso*-to-*meso* ethyne-bridged bis(porphinato)zinc(II) complex (directly analogous to **III** except that the porphyrin-pendant phenyl rings bear further substitution) shows that the two porphyrin macrocycles are coplanar; solid-state optical spectroscopic studies evince that this species exhibits a slightly red-shifted, narrower and more symmetric absorption band in the Q-band region with respect to what is observed for **III** (Figure 1).[36b] This observation is informative and suggests that the dominant low-energy component in the solution spectrum arises from a coplanar structure; moreover, it is consistent with the hypothesis that, in addition to the existence of vibronic states, at least a portion of the spectral heterogeneity observed in the Q-band region for compounds **III** and **IV** can be attributed to the presence of additional, presumably nonplanar conformers in solution which absorb at slightly higher energy than isomeric forms in which the (10,20-diphenylporphinato)zinc(II) units share an approximately coplanar relationship.

IV.b. Subpicosecond Dynamics. We now consider the factors governing the ultrafast dynamics of the (porphinato)-zinc(II) monomers, **ZnTPP** and *meso*-trimethylsilylethynyl elaborated **I**, and contrast them with the determinants of the early time dynamics observed for the β-to-β and *meso*-to-*meso* ethyne-bridged (porphinato)zinc(II)-based arrays **II**−**IV**. The observed, relatively slow, ~1 ps $S_2 \rightarrow S_1$ internal conversion for **ZnTPP** has been attributed to unfavorable Franck−Condon factors for nonradiative decay between parallel S_2 and S_1 potential energy surfaces, correlating with the relatively intense Q(1,0) transition for this complex;[31] the optical properties of **I** are consistent with similar Franck−Condon overlap of its S_2 and S_1 surfaces and the observation of a comparably slow internal conversion rate ($\tau = 0.9$ ps). In our experiments, the subpicosecond dynamics observed for **I** reveal a decay of the transient absorption anisotropy to a final value of ~0.1 on a time scale of $\tau = 350$ fs, which is faster than internal conversion. The depolarization dynamics for an $x-y$ degenerate electronic state may be rationalized within the context of a stochastic model,[33,38] which describes the role of solvent-induced energy and coupling fluctuations in determining both the rates of dephasing and population transfer between degenerate or nearly degenerate energy levels. In the present case, the experimental anisotropy does not contain any indication of $x-y$ coherence (i.e., values of $r(0) > 0.4$ or < -0.2);[29,33] we therefore conclude that dephasing is complete on a time scale faster than the temporal resolution of these measurements. The 350 fs depolarization of the anisotropy observed for **I** is caused by incoherent transfer of population between the B_x and B_y components of the E_u excited state, which are coupled by the random electric fields established by the fluctuating solvent environment; similar effects were observed within the *x*- and *y*-polarized S_1-excited states of MgTPP,[29] where equilibration between the *x* and *y* components occurred on a time scale of 1600 fs. It is important to note that depolarization will also result from internal conversion between orthogonal components of the S_2 and S_1 states. The observed 0.9 ps internal conversion time scale determined from our magic angle measurements carried out for compound **I** reflects the sum of the rates of all relaxation pathways between components of the S_2 and S_1 levels and hence does not provide information regarding the rate constants of the individual processes.

(36) (a) This argument is further bolstered by the fact that X-ray crystallographic studies of an analogue of compound **III** which possesses solublizing groups at the 4′-*meso*-phenyl positions show that the two (porphinato)zinc(II) macrocycles are mutually coplanar in the solid state. (b) Miller, D. C.; Shediac, R.; Carrol, P. J.; Therien, M. J. Manuscript in preparation.

(37) (a) Priyadarshi, S.; Beratan, D.; Therien, M. J. Unpublished results. (b) Shediac, R.; Lin, V. S.-Y.; Gray, M. H. B.; Karki, L.; Hupp, J. T.; Angiolillo, P. J.; Therien, M. J. Manuscript in preparation.

(38) Wynne, K.; Hochstrasser, R. M. *J. Raman Spectrosc.* **1995**, *26*, 561−569.

The isotropic and anisotropic transient dynamics observed for the β-to-β ethynyl-bridged dimer **II** stand in sharp contrast to that observed for compound **I**. Formation of the emitting state occurs on a faster time scale ($\tau = 150$ fs) for **II** than for the *meso*-ethynyl monomer; we note that a similar observation was made for a porphyrin μ-oxo dimer,[39] which was ascribed to an energy-transfer process that occurred between the B- and Q-states of adjacent chromophores. Clearly, the strong splitting observed in the B-band region of the dimer indicates a significant perturbation of the B-state electronic wave functions, while the absence of any perceptible splitting in the Q-band region suggests that the Q-states of the dimer are only weakly perturbed relative to the monomer.[7,23] These observations suggest that the Franck−Condon factors for B → Q internal conversion in the β-to-β ethyne-bridged dimer may be substantially different from those for the monomer, and hence possibly more favorable for nonradiative $S_2 \rightarrow S_1$ decay. Additionally, the splitting of the component levels of the S_2 manifold (Figure 1) establishes a band of intermediate levels between the state accessed by 400 nm excitation and the emitting state. This provides a "ladder" for sequential relaxations between successive pairs of levels that are separated by energies much smaller than the S_2-S_1 gap of conventional porphyrin monomers and less strongly coupled porphyrinic arrays (typically 7000−10000 cm^{-1}). Following formation of the emitting state of the β-to-β ethyne-bridged dimer, the ensuing subpicosecond dynamics are observed exclusively in the anisotropy (manifest as a ~650 fs decay) and do not appear in the magic angle signal, indicating transitions between spectrally identical states. This anisotropy decay is believed to originate from two processes. The first process corresponds to equilibration between the degenerate *x*- and *y* components of the S_1 state of a single porphyrin moiety within the dimer; such equilibration was previously determined to occur on a 1−2 ps time scale for 5,10,15,20-(tetraphenylporphinato)magnesium(II).[29] The second pathway by which the anisotropy can decay is by incoherent energy hopping between S_1 states of the porphyrin components of the dimer; while the mechanism of such an energy-transfer process is not probed directly in these experiments, it is important to note that Forster energy migration between halves of the dimer[40] would be expected to occur on a 100 fs-to-ps time scale. The final anisotropy value of ~0.05 is consistent with equilibration among states with noncoplanar transition moments, as expected for an orthogonal orientation of the porphyrin rings for the β-dimer.[7b]

The fast, instrument-response-limited rise of transient gain observed for the *meso*-to-*meso* ethyne-bridged bis- and tris-(porphinato)zinc(II) complexes signals the formation of the emitting states for these systems on a sub-100 fs time scale. Likewise, this facile internal conversion process may be facilitated by improved Franck−Condon factors, with respect to the monomeric building blocks and/or from the fact that the highly-split S_2 levels for compounds **III** and **IV** provide a large number of closely spaced intermediate states that enhance this process. The fact that the $S_2 \rightarrow S_1$ internal conversion process for compounds **III** and **IV** is faster than that observed for **II** is consistent with previously reported absorptive, emissive, electrochemical, and photoactivated triplet EPR spectroscopic data,[7,23] which evince that cylindrically π-symmetric groups that bridge porphyrins via a *meso*-to-*meso* linkage topology give rise to oligopigment systems exhibiting extraordinary ground- and excited-state electronic coupling between the constituent chromophores of the array.[7] The anisotropy measurements demonstrate that excitation at 400 nm is predominantly resonant with a transition that is orthogonal to the $S_1 \rightarrow S_0$ emission for both the dimer and trimer: this is entirely consistent with the expected splitting between *x* and *y* states and the stabilization of *x*-polarized transitions resulting from the *meso*-to-*meso* ethynyl linkage. The absence of any subpicosecond dynamics in the time-dependent anisotropy for both the *meso*-to-*meso* ethyne-bridged dimer and trimer, coupled with the measurement of a value of the anisotropy ($r \approx 0.4$) for 800 nm excitation of the tris(porphinato)zinc(II) complex **IV**, provides further support for significant splitting of *x*- and *y*-polarized transitions and the nondegenerate nature of the emitting states for these species, underscoring the distinctly different photophysics of these species with respect to that observed for **ZnTPP**, **I**, and **II**.

IV.c. Picosecond Dynamics. The emitting states of the monomeric porphyrins studied here are formed with a ~1 ps time constant following Soret photoexcitation and decay on a slow, >1 ns time scale. Dissipation of excess vibrational energy in similar closed-shell metalloporphyrin monomers has been observed to lead to spectral evolution on a 10−20 ps time scale.[30] Because the $S_2 \rightarrow S_1$ internal conversion will initially populate higher vibrational levels of the emitting state, assignment of the weak 18 ps component in the transient dynamics of the monomeric (5-trimethylsilylethynyl-10,20-diphenylporphinato)zinc(II) complex (**I**) to a vibrational cooling process in the S_1 state is sound. A similar 18 ps component is observed in the magic angle signal of the β-to-β ethyne-bridged dimer (**II**), which is consistent with a vibrational relaxation event; the fact that the vibrational cooling time constants are identical for **I** and **II** is congruent with the fact that **II**'s Q states are only slightly perturbed relative to those of **ZnTPP**.[7]

The dimer and trimer that possess the *meso*-to-*meso* ethyne-bridged linkage topology exhibit a dynamic red shift of the transient gain on a 30−35 ps time scale which is slower than is typically observed for excited-state vibrational cooling in porphyrins. It is interesting to hypothesize that this observed spectral signal corresponds to a dynamical process in which a population of nonplanar conformers evolves into a single S_1 emitting state in which the porphyrin macrocycles of these arrays share a coplanar spatial relationship; similar dynamics have been implicated in the ultrafast photophysics of oligothiophenes.[41] Consistent with the larger size of the porphyrin chromophore, the dynamics associated with this process for compounds **III** and **IV** occur on a time scale 7 times longer than that reported for thiophene oligomers. Examination of the time-resolved data obtained upon 400 nm excitation of **III** and **IV** (Figures 5−8) clearly shows that excitation at this wavelength accesses a state that is predominantly polarized orthogonal to the emitting state; the fact that the picosecond time domain anisotropy data show $r \approx -0.1$ indicates that an *x*-polarized state absorbs weakly at 400 nm as well (see section IV.a of the Discussion). Following rapid, subpicosecond internal conversion to the S_1 state, conversion of the nonplanar excited-state population to the maximally conjugated planar emitting state is reflected in the decay of transient gain at shorter wavelength (consistent with higher energy emission from a non-planar conformer), with a concomitant rise of transient gain at longer wavelength, corresponding to emission from a maximally conjugated planar structure. Such dynamics are however absent upon direct excitation of the emitting state of the trimer at 800 nm (Figure 9); we ascribe this to the direct excitation of the $S_0 \rightarrow S_1$

(39) Ohno, O.; Kaizu, Y.; Kobayashi, H. *J. Chem. Phys.* **1985**, *82*, 1779−1787.

(40) Kim, Y. R.; Share, P.; Pereira, M.; Sarisky, M.; Hochstrasser, R. M. *J. Chem. Phys.* **1989**, *91*, 7557−7562.

(41) Lanzani, G.; Nisoli, M.; Magni, V.; De Silvestri, S.; Barbarella, G.; Zambianchi, M.; Tubino, R. *Phys. Rev. B* **1995**, *51*, 13770−13773.

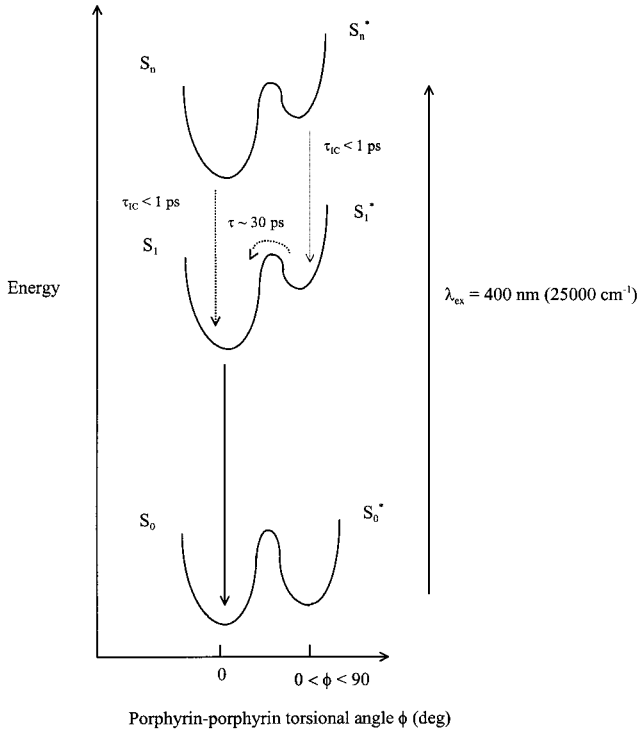

Figure 10. Schematic representation of the potential surfaces for the S_0, S_1, and S_2 states of the *meso*-to-*meso* ethyne-bridged dimer and trimer (**III** and **IV**) viewed along an inter-ring torsional coordinate (τ_{IC} = time constant for internal conversion).

absorption of a planar population of the *meso*-to-*meso* ethyne-bridged tris[(porphinato)zinc(II)] complex. On the basis of these observations and the results discussed in section IV.a, we propose a scheme for the potential energy surfaces that describe the ground and excited states of compounds **III** and **IV** (viewed along an inter-ring torsional coordinate) as shown in Figure 10. Selective excitation of the planar form of the dimer or trimer is possible when these species are optically pumped on the red side of the lowest energy Q-band absorptions shown in Figure 1 (λ_{max} for the absorption of the planar conformers corresponds to ~715 nm for **III** and 800 nm for **IV**); 400 nm excitation, however, is likely resonant with *x*- and *y*-polarized S_2 states corresponding to both planar and nonplanar conformers. Following fast internal conversion to their respective emitting states (denoted S_1 and S_1* in Figure 10), conversion from the nonplanar to planar form for **III** and **IV** occurs on a ~30 ps time scale as reflected by the slow dynamic red shift of emission. While still an open question, it is possible that the 700 fs component observed in the time-resolved dynamics for the *meso*-to-*meso* ethyne-bridged dimer **III** represents slower $S_2 \rightarrow S_1$ internal conversion for a population of non-planar conformers (Figures 5 and 6; see also the Supporting Information).

Comparison of the steady-state absorption and emission band shapes for the *meso*-to-*meso* ethyne-bridged chromophore systems reveals the emission profile to be narrow and relatively symmetric,[7] consistent with quenching of the high-energy fluorescence due to the proposed conformational change and further supporting the model discussed above. Steady-state and time-resolved measurements thus suggest that while a significant population of maximally conjugated planar structures exist for **III** and **IV** at ambient temperature in solution, a distribution of nonplanar conformers for these *meso*-to-*meso* bridged systems are also present; these different conformers manifest distinct excited-state dynamics which can be independently probed as a function of excitation wavelength. Although a similar origin for the 18 ps component observable in the transient dynamics for the β-to-β ethyne-bridged dimer cannot be ruled out, we believe this to be unlikely for the following reasons: (i) Steric factors are expected to restrict **II**'s structure to a narrow distribution of conformations at ambient temperature in which the constituent (porphinato)zinc(II) units are approximately orthogonal.[7b] (ii) No evidence is seen in **II**'s steady-state Q-band spectral absorption region to suggest conformational heterogeneity. Thus, if significantly different ground-state conformers for **II** existed, they would be required to be spectrally indistinguishable, which is a highly unlikely supposition.

It is interesting to note that a *meso*-to-*meso* vinyl-bridged bis(porphyrin) system, *trans*-bis[(5,5′;2,3,7,8,12,13,17,18-octaethylporphyrin)]ethene, exhibits unusual photophysical properties with respect to its 2,3,7,8,12,13,17,18-octaethylporphyrin building blocks; moreover, the excited-state dynamics of this species differs substantially from that described herein for *meso*-to-*meso* ethynyl linked compounds **III** and **IV**. Chachisvilis, Sundström, and co-workers reported the observation of rapid deactivation ($\tau \sim 7$ ps) of the S_1 excited state of *trans*-bis-[(5,5′;2,3,7,8,12,13,17,18,-octaethylporphyrin)]ethene.[42] From analysis of steady-state and time-resolved optical measurements, they concluded that (i) at least two conformers of the dimer are present in the S_0 state that differ with respect to the degree of coplanarity of their constituent 2,3,7,8,12,13,17,18-octaethylporphyrin rings and (ii) a *trans*-stilbene-like photoisomerization occurs on the S_1 surface that is followed by conformational relaxation and rapid internal conversion back to S_0. According to their model, the minimum of the S_1 state potential surface (viewed along the ethene C═C torsional coordinate) occurs at a dihedral angle that is intermediate to that of the two conformers; a barrierless pathway leads into this geometry following excitation of either of the ground-state conformers. The ground-state properties of the ethene- and ethyne-bridged systems thus are similar in that their optical spectra denote a conformational heterogeneity; they differ in the fact that, at ambient temperature in solution, the coplanar conformers of **III** and **IV** dominate the low-energy features of the optical spectrum, while the analogous maximally conjugated conformer for *trans*-bis[(5,5′;2,3,7,8,12,13,17,18-octaethylporphyrin)]ethene accounts for only a *minor* fraction of the observed absorptive oscillator strength. Furthermore, *the excited-state dynamics of trans*-bis[(5,5′;2,3,7,8,12,13,17,18-octaethylporphyrin)]ethene *contrast markedly with respect to meso-to-meso ethyne-linked compounds **III** and **IV**, indicating fundamental differences exist between their respective* S_1 potential energy surfaces. Clearly for **III** and **IV**, a low barrier exists for the conversion of nonplanar S_1-excited state populations to the lower energy, maximally conjugated planar S_1 emitting state. Importantly, the ~1 ns time scale of the $S_1 \rightarrow S_0$ radiative conversion observed for the low-energy emitting structure of ethyne-bridged systems **III** and **IV** highlights the potential for such porphyrin arrays in biomimetic photoconversion schemes, and stands in stark juxtaposition to the rapid deactivation and low emission quantum yields observed for *trans*-bis[(5,5′;2,3,7,8,12,13,17,18-octaethylporphyrin)]ethene.

Conclusions

The transient spectral data reported herein reveal a number of unusual photophysical properties with respect to those

(42) (a) Chachisvilis, M.; Chirvony, V. S.; Shulga, A. M.; Källebring, B.; Larsson, S.; Sundström, V. *J. Phys. Chem.* **1996**, *100*, 13857−13866. (b) Chachisvilis, M.; Chirvony, V. S.; Shulga, A. M.; Källebring, B.; Larsson, S.; Sundström, V. *J. Phys. Chem.* **1996**, *100*, 13867−13873.

elucidated previously for other classes of multiporphyrin systems. (i) The ultrafast, $S_2 \rightarrow S_1$ nonradiative relaxation rates manifest for these ethyne-bridged bis- and tris(porphinato)-zinc(II) complexes are at least an order of magnitude faster than observed for monomeric (porphinato)zinc(II) species, and increase with the extent of porphyrin−porphyrin electronic coupling in these complexes. (ii) The characteristics of the subpicosecond dynamics are clearly influenced by the mode of the porphyrin-to-porphyrin linkage topology; we have shown that the nature of the initially prepared excited states, as well as the states that are accessible in the ultrafast time domain, can vary from equilibrated, weakly-coupled localized degenerate states to those that are highly polarized and nondegenerate. (iii) The spectral evidence indicates that excited states for *meso*-to-*meso* ethyne-bridged bis- and tris[(porphinato)zinc(II)] systems **III** and **IV** can be initially prepared which are either structurally isomorphous or structurally distinct from that of the lowest energy emitting state. (iv) The picosecond time domain spectral evolutions evinced for compounds **III** and **IV** are both excitation-wavelength-dependent and consistent with conversion of nonplanar S_1-excited state conformers to a maximally conjugated emitting state over a 30−35 ps time scale.

The ability to modulate the ultrafast photodynamics and optical properties of these systems through the nature of the porphyrin-to-porphyrin linkage topology parallels the versatility seen in pigment−protein complexes which participate in biological light-harvesting and electron-transfer processes. This work suggests that oligomeric and polymeric porphyrin systems featuring macrocycle-to-macrocycle cylindrically π-symmetric bridges comprise ideal candidates for construction of multichromophoric assemblies for harvesting energy under specific optical conditions and rapidly transferring the excitation (or charge) in a directional fashion over long distances.

Acknowledgment. R.M.H. acknowledges the support of research grants from the National Science Foundation and the National Institutes of Health (NIH), and the NIH Research Resource Grant. M.J.T. is indebted to the NIH (Grant GM 48130-01A1.4) and the MRSEC Program of the National Science Foundation (Grant DMR-96-32598) for their research support, and to the Searle Scholars Program (Chicago Community Trust), the Arnold and Mabel Beckman Foundation, E. I. du Pont de Nemours, and the National Science Foundation for Young Investigator Awards, as well as to the Alfred P. Sloan and Camille and Henry Dreyfus Foundations for research fellowships. R.K. is the recipient of a postdoctoral fellowship (Grant F32 GM 16821) from the NIH.

Supporting Information Available: Figures showing picosecond isotropic transient dynamics and fits for **I** and **II** and time-dependent anisotropy for **III** and **IV** (5 pages, print/PDF). See any current masthead page for ordering information and Web access instructions.

JA981811U